Maximum Hydrostatic Stress Analysis of Multi-Pass Inclusion Copper Wire Drawing by FEM

Somchai NORASETHASOPON*

**Department of Mechanical Engineering, Faculty of Engineering,
King Mongkut's Institute of Technology, Ladkrabang, Bangkok, Thailand**

ABSTRACT

The size and length effects of inclusion on multi-pass copper shaped-wire drawing were investigated. The wire and inclusion deformations and hydrostatic stress of copper shaped-wires that contain an inclusion were calculated by two-dimensional finite elemental analysis. During drawing if a wire contains an inclusion, a necking occurred. The effects of inclusion size and length on maximum hydrostatic tensile stress in front of inclusion during multi-pass copper shaped-wire drawing were carried out. The maximum hydrostatic tensile stress appeared on the wire centerline in front of the inclusion for single-pass drawing. For multi-pass drawing, the maximum hydrostatic tensile stress was located at both sides of the wire centerline in front of the inclusion. Symmetrical double cracks easily originated in those regions.

Keywords: Multi-pass drawing, internal fracture, wire fracture, FEM, copper shaped-wire, inclusion, hydrostatic stress

*To whom correspondence should be addressed :
E-mail address: knosomch@kmitl.ac.th; Tel: (662) 326 4197; Fax: (662) 326 9053

INTRODUCTION

Drawing through dies can produce various solid cross-sections with various profiles. The initial cross-section is usually round or square. Proper die design and the selection of reduction sequence per pass require considerable experience to ensure proper material flow in the die in order to reduce defects and improve surface quality.

Table 1 Material properties and drawing conditions used for FEA

			Copper (wire)	WC (inclusion)
Young's modulus	E	(MPa)	120000	1000000
Yield stress	Y	(MPa)	150	1000
Poisson's ratio	ν		0.3	0.22
Die half-angle	α	(deg)	8	
Reduction per pass	R/P	(%)	20	
Coefficient of friction	μ		0.05	

As in all metalworking processes, successful drawing operations require careful selection of process parameters and consideration of many factors (Rao, 1999; Kalpakjian, 1995; Johnson, 1979; and Goetsch, 1991). Drawing speeds depend on the material and cross-sectional area. They may range form 1 m/s to 2.5 m/s (200 ft/min to 500 ft/min) for heavy sections to as fast as 50 m/s (10,000 ft/min) for very fine wire, such as that used for electromagnets. Because it does not have sufficient time to dissipate, the temperature can rise substantially at high drawing speeds and can have detrimental effects on the product quality.

Reductions in cross-sectional area per pass range from near zero to about 45 percent. Usually, the smaller the cross-section is to begin with, the smaller will be the reduction per pass. Fine wires are usually drawn at 15-25 percent reduction per pass, and larger sizes at 20-45 percent. Reductions of more than 45 percent may result in lubrication breakdown and surface-finish deterioration. Drawing large solid or hollow sections can be done at elevated temperatures. A light reduction called a sizing pass may also be taken on rods to improve the surface finish and dimensional accuracy. However, because they basically deform the surface layers, the light reductions usually produce highly non-uniform deformation of the material and its microstructure. Consequently, the properties of the material vary with location in the cross-section.

Because of work hardening, intermediate annealing between passes may be necessary to maintain sufficient ductility during cold drawing. Drawn copper John, (1999) and brass wires are designated by their temper, such as ¼ hard, ½ hard, etc. High-carbon steel wire for springs and musical instruments are made by heat treating, or patenting the drawn wires, whereby the microstructure obtained is fine pearlite. These wires have ultimate tensile strengths as high as 5 GPa (700 ksi) and tensile reduction of area of about 20 percent.

Basic Theory

The wire drawing processes are classified as indirect compression processes, in which the major forming stress results from the compressive stresses as a result of the direct tensile stress exerted in drawing (Mielnik, 1991). The converging die surface in the form of a truncated cone is used. The analytical or mathematical solutions are obtained by the freebody equilibrium method. By summing the forces in the wire drawing direction of a freebody equilibrium diagram of an element of the wire in the process of being reduced. Then combining the yield criterion with the equation for the axial force, integrating the resulting differential equation, and simplifying, the equation for the average drawing stress is obtained. In the derivation of this equation for drawing for a constant shear factor, neither a back pull stress nor the redundant works were included. These terms may be added, respectively, to give the equation for the front pull stress for drawing.

The above mentioned equations are only used for homogeneous wire drawing investigations. But non- homogeneous wire drawing such as wire drawing which contained an inclusion is a more complicated problem to investigate by those simple equations. In this case, the behaviors of wire drawing with an inclusion are easily investigated by two-dimensional FEA as presented in this paper.

The finite element method has become a powerful tool for the numerical solution of a wide range of engineering problems (Chandrupatla, 1991). With the advance in computer technology, a complex problem can be modeled with relative

ease. Several alternative configurations can be tried out on a computer before the first prototype is built. First step, Shape Functions, the finite element method expresses the unknown field in terms of the nodal point unknowns by using the shape functions over the domain of the element. Second step, Material Loop, the finite element method expresses the dependent flux fields such as the strain or stress in terms of the nodal point unknowns. Third step, Element Matrices, the finite element method equilibrates each element with its environment. Fourth step, Assembly, the finite element method assembles all elements to form a complete structure in such a manner to equilibrate the structure with its environment. Fifth step, Solve Equations, the finite element method specifies the boundary conditions, namely, the nodal point values on the boundary and the system equations are partitioned. Sixth step, Recover, the finite element method recovers the stresses by substituting the unknown nodal values found in 5th step back into 2nd step to find the dependent flux fields such as strain and stress.

FEM Results and Discussion

A two-dimensional finite element method was used to analyze the effect of an inclusion on copper shaped-wire drawing. Figure 1 shows the analytical model that was used. The black part was an inclusion in a copper shaped-wire. The inclusion was located at the center axis of the copper shaped- wire. The authors assumed that the inclusion was a sintered hard alloy (WC) Yoshida, (1982), Chen, *et al.* (1979), and Tanaka, *et al.* (1979) and have the material properties and drawing conditions used in this analysis as shown in Table 1. The inclusion length was set to be L_i/D_o, the ratio of inclusion length to dimension of wire cross section, and varied as 0.05, 0.1, 0.2, 0.3 and 0.4. The inclusion size was set to be D_i/D_0, the ratio of inclusion dimension to dimension of wire cross section, and varied as 0.1, 0.2, 0.3, and 0.4. The die half-angle (α), reduction per pass (R/P) and coefficient of friction (μ) were set at 8 degrees, Norasethasopon, (2001) 20%, and 0.05, Yoshida, (1982) respectively. The authors assumed that the inclusion and the copper
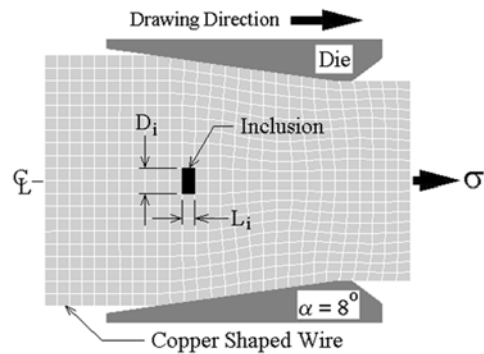
Figure 1 Model of copper shaped-wire contain an inclusion used in this analysis

matrix were joined at the boundary, and that the materials used were not work-hardened during the process. In this analysis, a wire was considered to be a copper shaped-wire containing a hard inclusion subjected to steady deformation.

For inclusion size (D_i/D_o) equal to 0.3 the distributions of hydrostatic stress and deformation behaviour of copper shaped-wires with an inclusion for non-dimensional inclusion length (L_i/D_o) equal to 0.05 during five-pass wire drawing were obtained as shown in Figure 2-6. The maximum hydrostatic tensile stress (σ_t/Y) of copper shaped-wires containing inclusions with $L_i/D_o = 0.05$ for $D_i/D_o = 0.1$, 0.2, and 0.4 were also obtained. As the inclusion passes through the die, necking due to an inclusion wire drawing occurred at some parts of the wire. The necking appeared on the copper shaped-wire surface in front of the inclusion near the inclusion
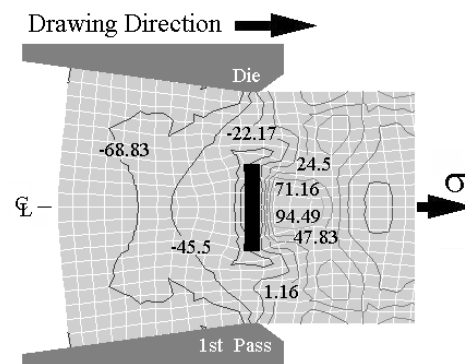
Figure 2 The distributions of hydrostatic stress and deformation behavior of copper shaped-wires with an inclusion for inclusion length (L_i/D_o) equal to 0.05 during 1st pass wire drawing
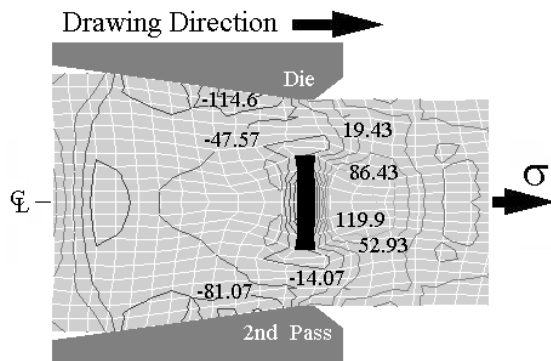
Figure 3 The distributions of hydrostatic stress and deformation behavior of copper shaped-wires with an inclusion for inclusion length (L_i/D_o) equal to 0.05 during 2nd pass wire drawing
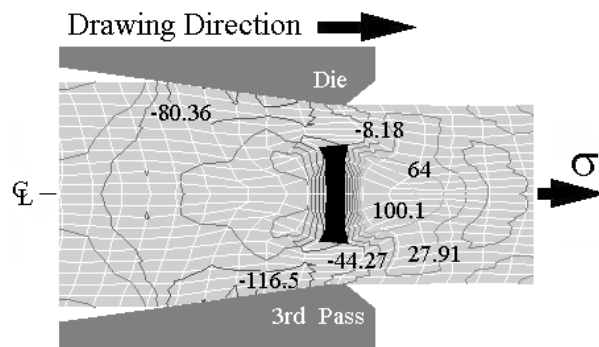
Figure 4 The distributions of hydrostatic stress and deformation behavior of copper shaped-wires with an inclusion for inclusion length (L_i/D_o) equal to 0.05 during 3rd pass wire drawing
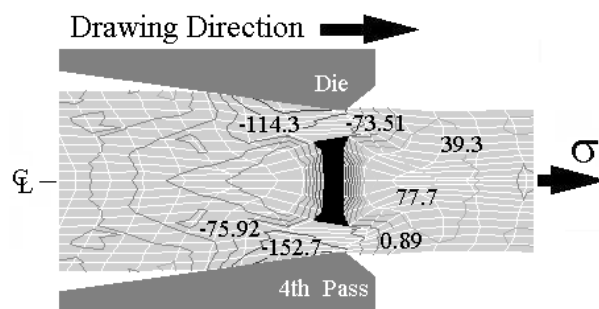
Figure 5 The distributions of hydrostatic stress and deformation behavior of copper shaped-wires with an inclusion for inclusion length (L_i/D_o) equal to 0.05 during 4th pass wire drawing
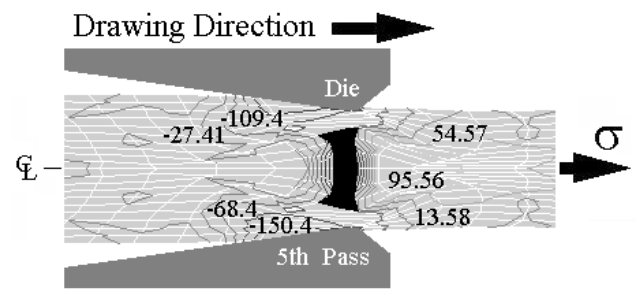
Figure 6 The distributions of hydrostatic stress and deformation behaviour of copper shaped-wires with an inclusion for inclusion length (L_i/D_o) equal to 0.05 during 5th pass wire drawing

boundary and its magnitude increased as D_i/D_o increased. During the drawing of wires containing an inclusion, it was found that σ_t/Y in front of the inclusion increased as D_i/D_o increased..

The inclusion front displacement (S_i/D_o) slightly influenced σ_t/Y. For third pass drawing Figure 4, the σ_t/Y in case of $D_i/D_o = 0.4$ was lower than the σ_t/Y as in the case of a smaller inclusion and was under very slight influence of S_i/D_o during the inclusion passing through the die. After the inclusion exits the die, the σ_t/Y increases until it is higher than σ_t/Y as in the case of smaller inclusions and highest at S_i/D_o equal to 0.13 then it decreases. The σ_t/Y in the case of all smaller inclusions increases as D_i/D_o increases. As D_i/D_o decreases, the highest σ_t/Y appeared where the inclusion front was out die and more far away from the die exit. For forth pass drawing, Figure 5 the σ_t/Y decreases as D_i/D_o increases and was slightly influenced by S_i/D_o during inclusion passing through the die. After the inclusion exits the die that behavior was inverted and the σ_t/Y increased as S_i/D_o increased until its highest point then it decreased. The highest σ_t/Y appeared where the inclusion front was out die and more far away from the die exit as D_i/D_o and S_i/D_o increased.

The maximum hydrostatic tensile stress increases as L_i/D_o increases. The inclusion front displacement (S_i/D_o) slightly influenced σ_t/Y for the first pass drawing, Figure 2 and influenced σ_t/Y for the second and third pass drawings Figure 3 and Figure 4. As L_i/D_o decrease, the highest σ_t/Y appeared where the inclusion front

was out die and more far away from the die exit. In the third pass drawing, a wire break occurred for L_i/D_o = 0.3 and 0.4. For the forth and fifth pass drawing, the σ_t/Y increased as L_i/D_o increased and was very slightly influenced by S_i/D_o during the inclusion passing through the die. After the inclusion exits the die, the σ_t/Y increases as S_i/D_o increases until its highest point then decreases. The highest σ_t/Y point appeared where the inclusion front was out die and more far away from the die exit as L_i/D_o decreased but S_i/D_o increased and wire break occurred for L_i/D_o = 0.2, 0.3 and 0.4.

For the first to third pass drawings, the maximum hydrostatic tensile stress (σ_t/Y) was located on the wire centerline. When the high σ_t/Y during wire drawing occurred, the internal central crack or chevron crack easily originated in this location. The L_i/D_o strongly influenced σ_t/Y for L_i/D_o approximately less than 0.2. The σ_t/Y rapidly increases as L_i/D_o and D_i/D_o increases. For L_i/D_o it was found that between 0.2 to 1.0, the L_i/D_o influenced σ_t/Y and influenced the transition of D_i/D_o from directly to inversely with respect to σ_t/Y. The σ_t/Y was not effected by L_i/D_o when L_i/D_o was approximately greater than 1.0. But D_i/D_o inversely strongly influenced σ_t/Y or in other words it increases as D_i/D_o decreases. For the forth and fifth pass drawings, the two symmetrically located maximum hydrostatic tensile stresses (σ_t/Y) were located on both sides of the wire centerline. In this case, the highest σ_t/Y increase and its location were out die and more far away from the die exit as repeated drawing times increased. The internal double symmetrical cracks easily originated in these two symmetrical regions.

CONCLUSIONS

1. Inclusion properties and wire properties influence the maximum hydrostatic tensile stress.

2. Necking due to an inclusion wire drawing occurred at some parts of the wire. The necking appeared on the copper shaped-wire surface in front of the inclusion near the inclusion boundary and inclusion size and length directly influenced its magnitude.

3. Maximum hydrostatic tensile stress increases as inclusion size increases for first and second pass drawing.

4. The inclusion front displacement slightly influenced the maximum hydrostatic tensile stress for first pass drawing and directly influenced the maximum hydrostatic tensile stress for second and third pass drawing.

5. The highest maximum hydrostatic tensile stress appeared where the inclusion front was out die and more far away from the die exit as inclusion length decreased.

6. The inclusion length was more influencial on the maximum hydrostatic tensile stress than the inclusion size.

7. In the first to third pass drawings, the inclusion front displacement was very slightly influencial on the maximum hydrostatic tensile stress.

8. The drawings pass strongly influenced the maximum hydrostatic tensile stress for forth and fifth pass drawings.

9. The maximum hydrostatic tensile stress was located on the wire centerline.

10. In the forth and fifth pass drawings, the inclusion front displacement strongly influenced the maximum hydrostatic tensile stress as a pulse relationship of maximum hydrostatic tensile stress and inclusion front displacement where the inclusion front exits the die and the inclusion front displacement was between 0.0 to 0.4.

11. The pulse relationship between maximum hydrostatic tensile stress and inclusion front displacement for inclusion size equal to 0.4 occurred, resulting in two symmetrically located maximum hydrostatic tensile stresses appearing on both sides of the wire centerline.

12. The highest maximum hydrostatic tensile stress for inclusion size equal to 0.4 appeared at an inclusion front displacement equal to 0.13 in third pass drawing. The maximum hydrostatic tensile stress that was located on these two symmetrical locations was very high. The internal double symmetrical cracks easily originated on these symmetrical locations. It also originated for all inclusion size in forth and fifth passes drawings.

13. The highest maximum hydrostatic tensile stress appeared where the inclusion front was out die and more far away from the die exit as inclusion size and inclusion front displacement increased but inclusion length decreased.

REFERENCES

John, Morton. 1999. Thomas Bolton & Sons and the rise of the electrical industry. *Eng. Sci. Educ. J.*

Yoshida, K. 1982. Doctor dissertation at Tokai Univ., Japan.

Chen, C. C., Oh, S. I. and Kobayashi, S. 1979. Trans. *ASME, Ser.B*. **101** : 23-44.

Tanaka, H. and Yoshida, K. 1979. *J. of the Japan Institute of Metals*. **43** : 618-625.

Raskin, C. 1997. Proceedings of the WAI International Technical Conference, Italy.

Mielnik, Edward M. 1991. *Metalworking Science and Engineering*. McGraw-Hill, Inc. New York : 397-462.

Norasethasopon, S. and Tangsri, T. 2001. Experimental Study of the Effect of a Half-Die Angle on Drawing Stress During Wire Drawing. *Ladkrabang Engineering Journal*. **18** : 134-139.

Chandrupatla, Tirupathi R. and Belegundu, Ashok D. 1991. *Introduction to Finite Elements in Engineering*. Prentice-Hall International, Inc. New Jersey.

Rao, P. N. 1999. *Manufacturing Technology Foundry, Forming and Welding*. McGraw-Hill, New Delhi.

Kalpakjian, Serope. 1995. *Manufacturing Engineering and Technology*. Addison Wesley, Massachusetts.

Johnson, Harold V. 1979. *Manufacturing Processes*. Bennett & McKnight, Encino, CA

Goetsch, David L. 1991. *Modern Manufacturing Processes*. Delmar Pub., N. P.